

# On Degeneracy of Linear Reconstruction From Three Views: Linear Line Complex and Applications

Gideon P. Stein and Amnon Shashua

**Abstract**—This paper investigates the linear degeneracies of projective structure estimation from line features across three views. We show that the rank of the linear system of equations for recovering the trilinear tensor of three views reduces to 23 (instead of 26) when the scene is a Linear Line Complex (a set of lines in space intersecting at a common line). The LLC situation is only linearly degenerate, and one can obtain a unique solution when the admissibility constraints of the tensor are accounted for. The line configuration described by an LLC, rather than being some obscure case, is in fact quite typical. It includes, as a particular example, the case of a camera moving down a hallway in an office environment or down an urban street. Furthermore, an LLC situation may occur as an artifact such as in direct estimation from spatio-temporal derivatives of image brightness. Therefore, an investigation into degeneracies and their remedy is important also in practice.

**Index Terms**—Shape representation and recovery, 3d motion and shape recovery from line correspondences, shape from motion, algebraic and projective geometry.

## 1 INTRODUCTION

It is known that point and line image features across three perspective views can generally give rise to a linear system of equations for a unique solution for 3D structure and camera motion. The structure and motion parameters are represented by a  $3 \times 3 \times 3$  tensor. The image measurements of matching points and lines provide constraints, trilinear in image coordinates, that as a whole make a linear system of equations for the (unknown) coefficients of the tensor. Finally, the tensor has only 18 degrees of freedom, i.e., the 27 coefficients are subject to nonlinear admissibility constraints. In the presence of errors in image measurements, one often starts with the linear solution and improves it further by employing a numerical Gauss-Newton style iterative procedure until a solution that satisfies the admissibility constraints is obtained. (See Appendix for more details.)

In this paper, we investigate the cases in which the linear solution is degenerate. As it happens, the degeneracy occurs in typical real situations. We show that when the sample of features is taken from a configuration of lines that have a common intersection, known as a Linear Line Complex (LLC), then the rank of the linear system reduces from 26 (in the general case) to 23—yet, there exists a *unique* solution for the tensor when the nonlinear admissibility constraints are accounted for. (This in contrast to *critical line configurations* from which a unique solution is not possible, see [6], [2], [8].) An LLC includes in particular the case of lines on parallel planes whose degeneracy was observed in [19].

To appreciate the practical importance of investigating LLC configurations, consider a few typical outdoor and indoor scene

examples depicted in Fig. 1. In Fig. 1a, the common intersecting line is the vertical edge of the building visible in the center of the image (“the corner”). All horizontal lines on the two faces of the building meet the edge in the image plane, and the vertical lines meet the edge at infinity. Note also that the vertical line representing the lamp-post also meets the edge of the building (at infinity) thereby included in the LLC configuration. This leaves very few lines (the sidewalk and the oblique line of the lamp-post) not part of the LLC. Imagine a robot moving down the hallway in Fig. 1b. The lines are either in the direction of motion or lie on a set of planes that are perpendicular to the direction of motion. The lines on the parallel planes all intersect a common line on the plane at infinity. As we will see the lines in the direction of motion also form a degenerate configuration.

Finally, an LLC situation occurs also as an artifact in direct estimation of the tensor from spatio-temporal derivatives of image brightness [17]. The spatiotemporal derivatives provide an axis of certainty (a one-dimensional uncertainty) for the location of the matching points in views 2, 3 relative to points in the reference view 1. The uncertainty axes in views 2, 3 are parallel which means that the information gathered from a *general* scene by means of first-order spatiotemporal derivatives is at most comparable to the information gathered from an LLC configuration of discrete matching lines.

Given our main result, an attempt to reconstruct structure and motion from the image line information of the scenes in Fig. 1 using conventional approaches would be at best unstable. The linear system of equations is singular or near singular, and would most likely not serve as a reasonable starting solution for a subsequent Gauss-Newton iterations. Therefore an investigation into degeneracies caused by an LLC and their remedy is important also in practice.

The remainder of the paper is organized as follows. Section 2 contains the main results which include the statement of degeneracy of the linear system forming a null space of dimension 4, and the statement of uniqueness by incorporating the admissibility constraints with a simple constructive algorithm for obtaining a unique solution from an LLC configuration. In Section 3, we discuss the dimension of the null space for a planar object of points, and in Section 4, we verify the theory and the algorithm with experiments with real images. In our experiments, we use a schematized model of the real scene shown in Fig. 1a because this allows for a wide set of experiments. In these images, one can accurately find both line and point correspondences and can therefore perform the motion estimation using line correspondences and then verify the results against motion estimates obtained using points.

Notations in general, and tensorial notations in particular, plus the theory and background of the Trilinear Tensor with its contraction and slicing properties and admissibility constraints are discussed in the Appendix.

## 2 LINEAR LINE COMPLEX SCENE STRUCTURE

Consider the tensor  $\mathcal{T}_i^{jk}$  applied to the point-line-line configuration:

$$s'_j s''_k (p^i) \mathcal{T}_i^{jk} = 0,$$

where  $p$  is a point in image 1 and  $s'$ ,  $s''$  are lines coincident with the matching point  $p'$ ,  $p''$  in image 2 and 3, respectively. Note that  $p^i \mathcal{T}_i^{jk}$  is a  $3 \times 3$  matrix determined by  $p$ , which we will denote by  $B_p$ , i.e., in matrix notation  $s''^T B_p s' = 0$  for all pairs of lines coincident with  $p', p''$ . Assume that there exists a matrix  $B$ , independent of  $p$ , such that  $s''^T B s' = 0$ , then clearly the tensor  $\mathcal{T}_i^{jk}$  is not unique: slice the tensor into three matrices  $(\mathcal{T}_1^{jk}, \mathcal{T}_2^{jk}, \mathcal{T}_3^{jk})$ , then the tensors  $(B, 0, 0)$ ,  $(0, B, 0)$ , and  $(0, 0, B)$  (and their linear combinations) all

• G.P. Stein is currently at the Artificial Intelligence Laboratory, Massachusetts Institute of Technology, Cambridge, MA 02139.  
E-mail: gideon@ai.mit.edu.

• A. Shashua is at the Institute of Computer Science, Hebrew University of Jerusalem, Israel. E-mail: shashua@cs.huji.ac.il.

Manuscript received 8 Dec. 1997; revised 10 Nov. 1998. Recommended for acceptance by B. Vemuri.

For information on obtaining reprints of this article, please send e-mail to: tpami@computer.org, and reference IEEECS Log Number 107781.



(a)



(b)

Fig. 1. Typical urban indoor and outdoor scenes. The lines in the images form a Linear Line Complex. See text for more details.

satisfy the constraint  $s'_j s''_k p^i T_i^{jk} = 0$ . Hence, such a matrix  $B$  does not exist in general. We may, nevertheless, ask *whether there exists a special configuration of points and lines in space for which such a matrix  $B$  is valid?* Such a configuration is a Linear Line Complex (LLC).

**THEOREM 1.** *Let  $S$  be a set of lines in 3D which have a common intersecting line  $L$  (i.e.,  $S \wedge L = 0$  for all  $S \in S$ ). Let  $Q$  be a set of lines in 3D that intersect the line joining the two camera centers. Then, there exists a unique matrix  $B$  satisfying  $s''^T B s' = 0$  for all pairs of projections  $s', s''$  of lines  $S \in S$  onto two distinct views. The matrix  $B$  also satisfies  $q''^T B q' = 0$  for all pairs of projections  $q', q''$  of lines  $Q \in Q$ .*

**PROOF.** Let  $P$  be the intersection of a line  $S \in S$  with  $L$  and denote its projections by  $p', p''$  onto views 2, 3, respectively (see Fig. 2). Choose any plane  $\pi$  from the pencil of planes meeting at the line  $L$ , and let  $H_\pi$  be the corresponding 2D projective mapping (homography matrix) of points in view 2 to points in view 3 via (projections of) the plane  $\pi$ . Since  $\pi$  contains the line  $L$ , then

$$H_\pi p' \cong p''.$$

Let  $l, l'$  be the projections of  $L$ , then  $p'$  is the intersection of  $s'$  and  $l$ , thus,

$$H_\pi [l]_x s' \cong p'',$$

where  $[l]_x$  denotes the skew-symmetric matrix of cross products, i.e.,  $p' \cong l \times s' = [l]_x s'$ . Likewise,  $s''$  is coincident with  $p''$ , then

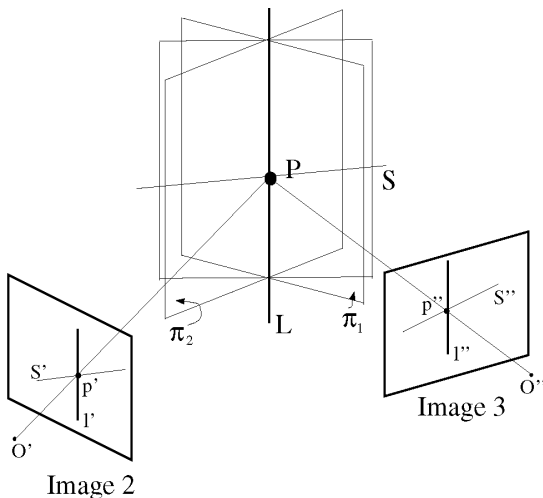


Fig. 2. Figure to accompany Theorem 1.

$$s''^T H_\pi [l]_x s' = 0.$$

Denote  $B_\pi = H_\pi [l]_x$ . We show next that  $B_\pi$  is unique, i.e., independent of the choice of  $\pi$ . Let  $\pi_1, \pi_2$  be two distinct planes of the pencil and let  $H_{\pi_1}, H_{\pi_2}$  be their corresponding homography matrices. It is known that any two homography matrices between two fixed views satisfy,

$$H_{\pi_2} \cong \lambda H_{\pi_1} + e'' n^T$$

where  $e''$  is the projection of the optical center of camera 2 onto the image plane of camera 3 (the epipole), and  $n$  is a free vector. Because  $\pi_1, \pi_2$  intersect at  $L$ , then,  $H_{\pi_2} u \cong H_{\pi_1} u$  for all  $u^T l = 0$ , thus  $n \cong l$  and we have:

$$H_{\pi_2} \cong \lambda H_{\pi_1} + e'' l^T,$$

and from which it clearly follows that  $B_{\pi_1} = B_{\pi_2}$ .

Let  $D$  be the intersection of a line  $Q \in Q$  with the plane  $\pi$  and denote its projections by  $d', d''$  onto views 2 and 3. The image line  $q'$  passes through the point  $d'$  and through the epipole  $e'$  and therefore:  $q' \cong e' \times d'$ . and similarly  $q'' \cong e'' \times d''$ . We can then write:

$$\begin{aligned} q''^T B q' &= (e'' \times d'')^T H [l]_x (e' \times d') \\ &= (e'' \times d'')^T H (d' \cdot l') e' - (e'' \times d'')^T H (l' \cdot e') d' \\ &= (d' \cdot l') (e'' \times d'')^T e'' - (l' \cdot e') (e'' \times d'')^T d'' \\ &= 0 \end{aligned} \quad (1)$$

where we used the identity:

$$a \times (b \times c) = (c \cdot a) b - (a \cdot b) c \quad (2)$$

and the fact that the homography  $H$  maps  $d'$  to  $d''$  and  $e'$  to  $e''$ .  $\square$

**COROLLARY 1.** *The rank of the estimation matrix of the tensor from image measurements of lines across three views of a Linear Line Complex structure is at most 23.*

**PROOF.** Let the tensor  $\mathcal{T}_i^{jk}$  be sliced into three matrices  $(\mathcal{T}_1^{jk}, \mathcal{T}_2^{jk}, \text{ and } \mathcal{T}_3^{jk})$ , then the tensors  $(B, 0, 0)$ ,  $(0, B, 0)$ , and  $(0, 0, B)$  (and their linear combinations) span the tensors of the form:

$$\mathcal{T}_i^{jk} = \delta_i b^{jk}$$

where  $\delta$  is a free vector of the family. Then,

$$s'_j s''_k p^i \mathcal{T}_i^{jk} = (p^i \delta_i) (s'_j s''_k b^{jk}) = 0.$$

Since  $\delta_i b^{jk}$  does not include the general form of trilinear tensors (4), the null space of the estimation matrix includes at least four distinct vectors: the true tensor describing the relative location of the three cameras, and the three ‘ghost’ tensors  $(B, 0, 0)$ ,  $(0, B, 0)$ , and  $(0, 0, B)$ . Thus, the rank is at most  $27 - 4 = 23$ .  $\square$

The ambiguity can be further reduced by incorporating the tensor admissibility constraints (see Appendix) as detailed below.

**THEOREM 2.** *The ambiguity of Tensor estimation from measurements coming from an LLC structure is at most an eight-fold ambiguity.*

**PROOF.** We assume the correlation matrix slicing of the tensor into the three standard correlation matrices ( $\mathcal{T}_1^{jk}$ ,  $\mathcal{T}_2^{jk}$ , and  $\mathcal{T}_3^{jk}$ ) (see Appendix). Let  $W$  be the  $N \times 27$ ,  $N \geq 27$ , estimation matrix for linear estimation of the tensor, i.e.,  $Wv = 0$  where  $v$  is the tensor whose elements are spread as a 27-element vector, and  $v$  is spanned by the four-dimensional null space of  $W^T W$ . Let  $v_1$ ,  $v_2$ ,  $v_3$  be the three ‘ghost’ tensors corresponding to  $(B, 0, 0)$ ,  $(0, B, 0)$ , and  $(0, 0, B)$ , respectively. Let  $v_0$  be the (one-dimensional) null space of

$$W^T W - v_1 v_1^T - v_2 v_2^T - v_3 v_3^T.$$

Since the null space spans the admissible tensors, the three standard correlation matrices ( $T_1$ ,  $T_2$ ,  $T_3$ ) of the admissible tensors are spanned by the tensors  $v_0, \dots, v_3$ , i.e.,

$$\begin{aligned} T_1 &= \hat{T}_1 + \alpha_1 B \\ T_2 &= \hat{T}_2 + \alpha_2 B \\ T_3 &= \hat{T}_3 + \alpha_3 B \end{aligned}$$

where  $\hat{T}_i, i = 1, 2, 3$ , are the standard correlation matrices of the tensor  $v_0$ , and  $\alpha_i$  are scalars. As part of the admissibility constraints (see Appendix), the standard correlation matrices  $T_i$  must be of rank 2, thus  $\alpha_i$  are generalized eigenvalues of  $\hat{T}_i$  and  $B$ , and since  $B$  is of rank 2, the characteristic equation for each  $\alpha_i$  is of second order. Thus, we have at most eight distinct solutions for  $T_i$ .  $\square$

**EMPIRICAL OBSERVATION 1.** Only one of the eight solutions satisfies all the admissibility constraints.

**EXPLANATION.** The rank-2 constraint of the standard correlation matrices is closed under linear superposition (see Appendix). Numerical experiments show that only one out of the eight possible solutions for the generalized eigenvalues  $\alpha_1, \alpha_2$ , and  $\alpha_3$  produces standard correlation matrices  $T_1, T_2, T_3$  whose linear superpositions produce rank-2 matrices.

## 2.1 Algorithm for Recovering Structure and Motion in the LLC Case

- 1) Using robust estimation techniques determines the line correspondences which belong to the LLC and compute the matrix  $B$  (see Theorem 1). Here one might use a robust version of the eight-point algorithm [4].
- 2) From the matrix  $B$ , create the three ‘ghost’ tensors:  $v_1 = (B, 0, 0)$ ,  $v_2 = (0, B, 0)$ , and  $v_3 = (0, 0, B)$ .
- 3) Using the point-line-line correspondences from the three views, compute  $W$ , the  $N \times 27$ ,  $N \geq 27$  estimation matrix for the linear estimation of the tensor.
- 4) Find  $v_0$ , the fourth vector spanning the (row) null space of  $W$  orthogonal to  $v_1, v_2$ , and  $v_3$  by finding the null space of:

$$W^T W - v_1 v_1^T - v_2 v_2^T - v_3 v_3^T.$$

In practice, take the eigenvector corresponding to the smallest eigenvalue.

- 5) Find scalars  $\alpha_i$  such that the vector:

$$v = v_0 + \sum_{i=1}^3 \alpha_i v_i$$

is an admissible tensor (see Theorem 2). This is done in two stages:

- Let  $\hat{T}_i, T_i, i = 1, 2, 3$ , be the standard correlation matrices of the tensors  $v_0$  and  $v_i$ , respectively. Then:

$$T_i = \hat{T}_i + \alpha_i B$$

Enforce the constraint that  $T_i$  is of rank-2 to find  $\alpha_i$ . Since the matrix  $B$  is of rank-2, this is a quadratic constraint resulting in up to two solutions for each  $\alpha_i$  for a total of  $2^3 = 8$  solutions.

- Prune the number of solutions down to one by enforcing the stronger admissibility constraint that any linear superposition of matrices  $T_i$  must be of rank-2. This is done by generating  $K$  random sets of linear coefficients  $\delta_i$  such that  $\sum \delta_i^2 = 1$  and computing the determinant of the linear superposition:  $\sum \delta_i T_i$  for each of the eight possible solutions. The solution that consistently gives  $\det(\delta_i T_i) \approx 0$  is the correct solution.

## 3 THE CASE OF PLANAR CONFIGURATIONS

Consider again the point-line-line contraction:

$$p^i s'_j (s''^k \mathcal{T}_i^{jk}) = 0.$$

Denote the matrix  $s''^k \mathcal{T}_i^{jk}$  by  $E_s$ , i.e., in matrix notation we have  $s'^T E_s p = 0$ . If there exists a matrix  $E$ , independent of  $s'$ , such that  $s'^T E p = 0$  for all lines  $s'$  coincident with the matching point  $p'$ , then clearly the tensor  $\mathcal{T}_i^{jk}$  is not unique: Slice the tensor into three matrices ( $\mathcal{T}_i^{j1}, \mathcal{T}_i^{j2}, \mathcal{T}_i^{j3}$ ), then the tensors  $(E, 0, 0)$ ,  $(0, E, 0)$ , and  $(0, 0, E)$  (and their linear combinations) all satisfy the constraint  $p^i s'_j s''^k \mathcal{T}_i^{jk} = 0$ . Hence, such a matrix  $E$  does not exist in general. However, if the matching points  $p, p'$  are projections of a coplanar configuration of points  $\pi$  in space and  $E$  is the corresponding homography matrix  $Ep \cong p'$ , then  $s'^T E p = 0$  for all lines  $s'$  coincident with  $p'$ .

Likewise, let  $W$  be the homography matrix due to  $\pi$ , i.e.,  $Wp \cong p''$ , then  $s''^T W p = 0$  for all lines  $s''$  coincident with  $p''$ . Then, given the slicing of the tensor into three matrices ( $\mathcal{T}_i^{1k}, \mathcal{T}_i^{2k}, \mathcal{T}_i^{3k}$ ), then the tensors  $(W, 0, 0)$ ,  $(0, W, 0)$ , and  $(0, 0, W)$  (and their linear combinations) all satisfy the constraint  $p^i s'_j s''^k \mathcal{T}_i^{jk} = 0$ .

Therefore, the rank of the null space of the linear system of equations for the tensor is at least six, since we have just created six ‘ghost’ tensors. The theorem below settles the question of whether the ghost tensors include the true tensor, in which case the rank of the estimation matrix is 21, or do not include the true tensor, resulting in a rank of 20.

**THEOREM 3.** *The rank of the estimation matrix of the tensor from image measurements of three views of a planar configuration of points is at most 21.*

**PROOF.** Denote the planar object by  $\pi$  and let  $E, W$  be the homography matrices due to  $\pi$  from view 0 to 1, and from view 0 to 2, respectively. The ‘ghost’ tensors due to  $E$  span the tensors of the form:

$$\mathcal{T}_i^{jk} = \delta^k e_i^j$$

where  $\delta$  is a free vector of the family. Then,

$$p^i s'_j s''^k \mathcal{T}_i^{jk} = (\delta^k s''^k) (p^i s'_j e_i^j) = 0.$$

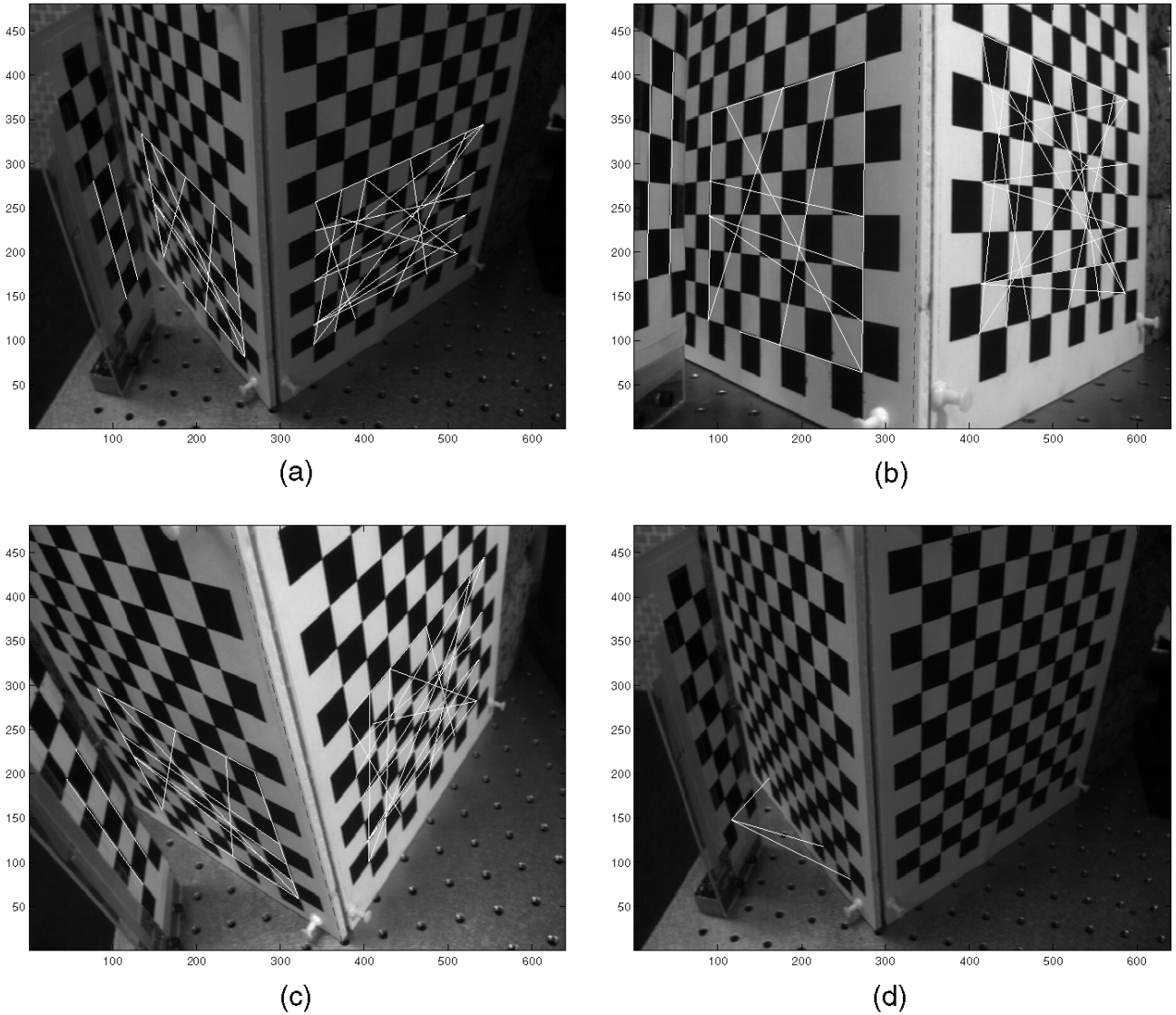


Fig. 3. The three input images used. All the lines marked are part of a linear line complex. They all intersect the line defined by the edge of the cube. Vertical lines intersect the edge at the point at infinity. The LLC was computed using (b) and (c). The dashed lines in (b) and (c) are the projection of the common intersection line into the images. The results show it aligns very well with the edge of the true cube. (d) Three lines which are not part of the LLC that are used in the experiments.

Likewise, the “ghost” tensors due to  $W$  span the tensors of the form:

$$\mathcal{T}_i^{jk} = \mu^j w_i^k$$

where  $\mu$  is a free vector of the family. Then,

$$p^i s'_j s'_k \mathcal{T}_i^{jk} = (\mu^j s'_j) (p^i s'_k e_i^k) = 0.$$

The six-dimensional null space spanned by both families of “ghost” tensors spans the tensors of the form:

$$\mathcal{T}_i^{jk} = \mu^j w_i^k + \delta^k e_i^j$$

where  $\delta, \mu$  are free vectors of the family. This family includes the true tensor (set  $\mu = v'$  and  $\delta = v''$ ). Thus, the rank of the estimation matrix is at most  $27 - 6 = 21$ .  $\square$

Note, that unlike the case of LLC in which the admissibility constraints have reduced the ambiguity to a single solution, here the null space includes admissible tensors (admissibility constraints are satisfied), thus a unique solution is not possible. The ambiguity is also evident by straightforward counting: the tensor is determined by 18 (algebraically independent) parameters, yet

two homography matrices ( $E, W$ ) give rise only to eight parameters each (because each matrix is up to scale), thus we have two parameters missing for uniquely determining the tensor from a planar surface.

## 4 EXPERIMENTS

### 4.1 The Experimental Procedure

Fig. 3a, Fig. 3b, and Fig. 3c show the three input images used for the experiments. The scene is composed of two faces of a cube and another plane on the left which is parallel to the vertical edge of the cube. This is a schematic model of a typical urban scene with an edge of a building such as in Fig. 1a.

Corresponding point features were manually extracted. The feature points were saddle points formed by the corners of two black squares which can be found with subpixel accuracy. The point features were grouped into four groups: Points from the left and right faces of the cube form one group each. Points on the planar surface were grouped into two vertical sets of features.

Line features were created by taking pairs of points. If no pair of points has members from more than one group (for example,

TABLE 1

VALUES OF THE ERROR COST FUNCTION FOR ESTIMATING THE LLC

Extra Line	$E_{23}$	$E_{12}$	$E_{13}$
None	0.000055	0.00064	0.000079
Close	0.0019	0.0016	0.00054
Middle	0.0065	0.0038	0.0017
Far	0.0119	0.0919	0.0062

When all the lines belong to the LLC (none) and when we add a line which passes close to or far from the common line of intersection (the edge of the cube).

Fig. 3), then we limit ourselves to a Linear Line Complex since all the 3D lines in the scene intersect the edge of the cube. By adding pairs that span two groups we can add lines that do not belong to the LLC. By judiciously choosing pairs we can add lines that are close or far from being part of the LLC (see Fig. 3d). We can also choose pairs of points that define lines passing through the epipoles. This flexibility allows us to verify all the claims in Theorem 1.

#### 4.2 Hardware Notes

The images were captured using a Pulnix TM9701 progressive scan camera with a 2/3 inch CCD and an 8.5 mm lens. The image resolution was  $640 \times 480$  pixels.

To achieve the results presented here, we had to take into account radial lens distortion. Only the first term of radial distortion was used. The radial distortion parameter,  $K_1 = 6e - 7$  was found using the method described in [18]. We note that that parameter value also minimized the error terms in (3).

#### 4.3 Determining the LLC

The three input images (Fig. 3a, Fig. 3b, and Fig. 3c) will denote image 1, 2, and 3, respectively. We chose  $N = 28$  pairs of points which defined lines all belonging to the LLC. These are overlaid as white lines in the figures. For each image pair (1, 2), (2, 3), and (1, 3), we used the eight-point algorithm [4] applied to the line correspondences to compute the matrices  $B_{12}$ ,  $B_{23}$ , and  $B_{13}$  that minimize:

$$\begin{aligned} E_{12} &= \frac{1}{N} \sum_{i=1}^N (s_i B_{12} s'_i)^2 \\ E_{23} &= \frac{1}{N} \sum_{i=1}^N (s_i B_{23} s''_i)^2 \\ E_{13} &= \frac{1}{N} \sum_{i=1}^N (s_i B_{13} s''_i)^2 \end{aligned} \quad (3)$$

respectively. The coordinates of the lines  $s$ ,  $s'$ ,  $s''$  have been scaled as described in [4]. From Theorem 1, the left and right null spaces of  $B_{23}$  (for example) are the projections of the line  $L$  in images 2 and 3. The dashed black line in Fig. 3b and Fig. 3c shows the lines corresponding to the null spaces overlaid on the input images. They align well with the edge of the cube verifying the theory and showing that the matrix  $B$  can be recovered accurately. Similar results were found using the other image pairs.

Fig. 3d shows image 1 on which we have overlaid three lines not belonging to the LLC. Table 1 shows the error terms of (3) when all the line are from the LLC and when we add one of the lines shown in Fig. 3d. When the extra line is far away from the common line of intersection, the error is large. Even when the line nearly intersects the edge of the cube, the error is still significant. Therefore, robust methods can be used for outlier removal if most of the lines come from from an LLC. Other experiments, not reported here, use lines that pass through the epipole to verify the second half of Theorem 1.

#### 4.4 Recovering Motion and Structure

We computed the motion tensor from the three views using four methods. First we used the linear method for a set of 131 point correspondences. Then we used the linear method for a set of 34 nondegenerate line correspondences. Next we applied the linear method in a naive way to the set of 28 line correspondences from an LLC. In other words, we ignored the fact that the lines come from an LLC. Finally, we estimated the tensor from the 28 degenerate lines using the algorithm described in Section 2.1.

##### 4.4.1 Condition of the Estimation Matrix

Fig. 4a (top) shows the four smallest singular values of the estimation matrix  $W^T W$  used to compute the tensor from 34 nondegener-

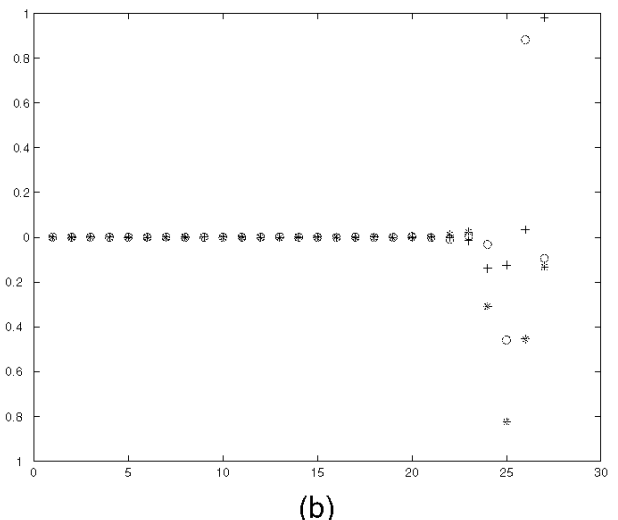
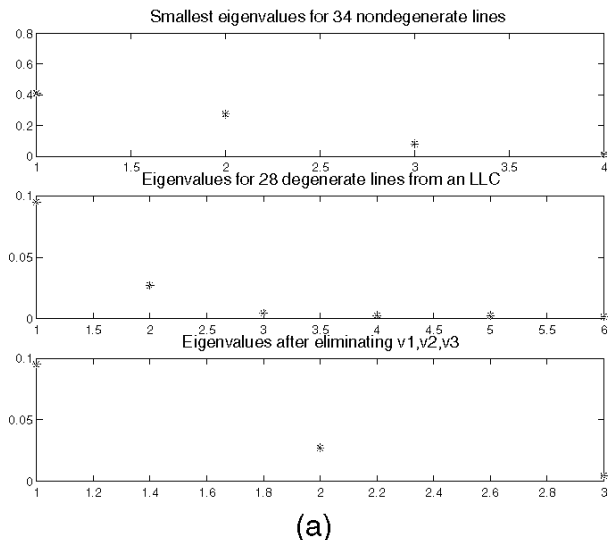


Fig. 4. (a) The smallest singular values of the estimation matrix  $W$  for a degenerate and nondegenerate set of lines. (b) With a degenerate set of lines, the vectors  $v_1$ ,  $v_2$ , and  $v_3$  were projected onto the 27 eigenvectors of  $W^T W$ . The values for the first 23 eigenvectors are close to zero verifying that the vectors  $v_1$ ,  $v_2$ , and  $v_3$  are orthogonal to the first 23 eigenvectors and are therefore in the null space of  $W^T W$ . (See Theorem 2.)

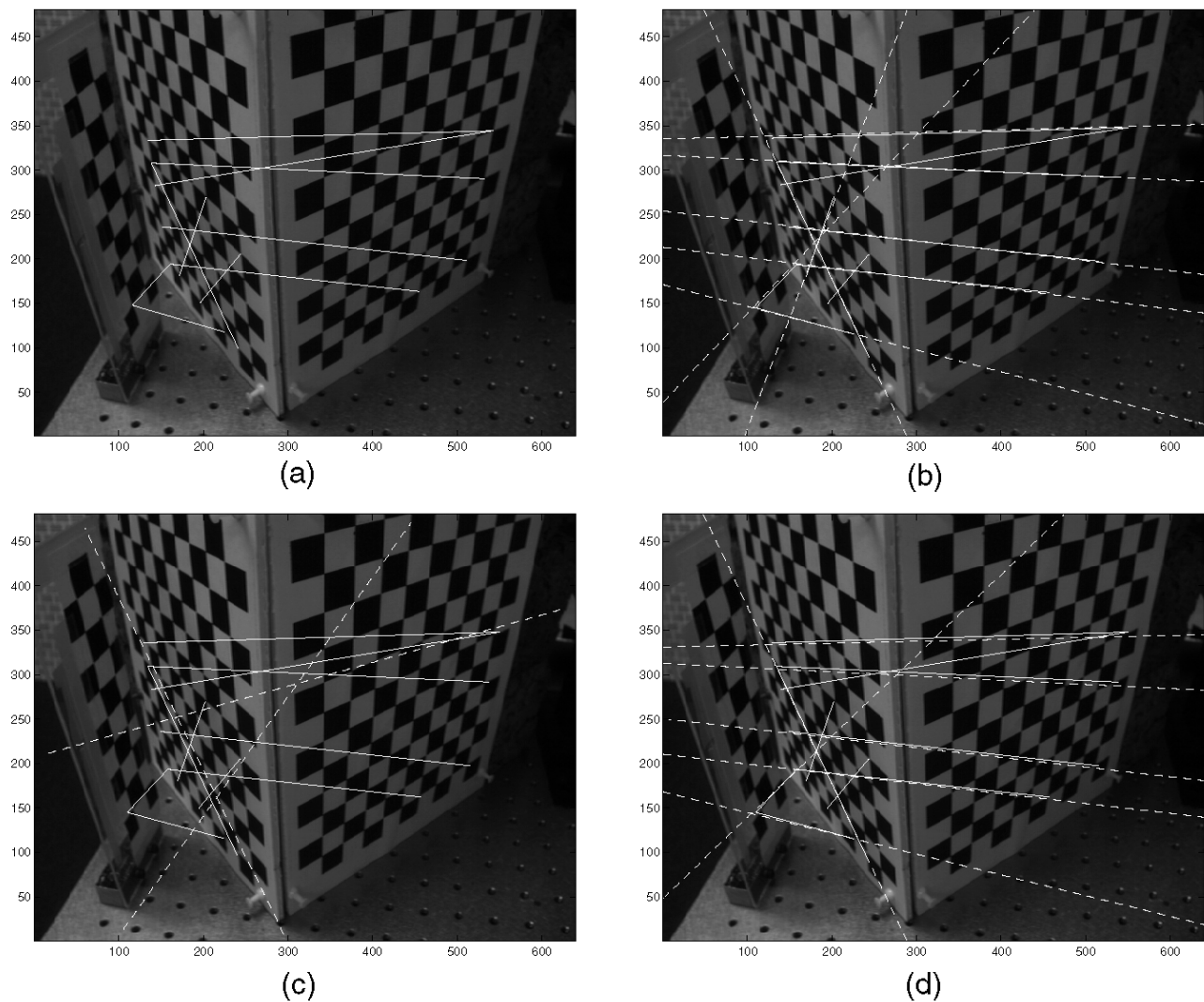


Fig. 5. (a) Ten additional lines are used to test the recovered tensors. Three of the lines lie on the left face of the cube and are therefore the part of the LLC. The other seven are not. The test lines from images 2 and 3 are reprojected back into image 1 using the recovered tensors. Solid lines are the true locations. Dashed lines are the reprojected lines. (b) The tensor was computed using a set of 34 nondegenerate lines. (c) The tensor was computed using a degenerate set of 28 lines using the standard method. Since it does not take into account the degeneracy, the tensor fails to correctly reproject the lines. The only lines in (c) that reproject correctly are those that belong to the LLC. (d) Using the new algorithm for the degenerate case, the computed tensor correctly reprojects all the lines.

ate lines. The smallest eigenvalue is considerably smaller than the others indicating that the null space of the matrix is of rank = 1 and the problem is well conditioned. Fig. 4a (middle) shows the five smallest singular values for the estimation matrix computed from 28 lines belonging to an LLC. The four smallest singular values are about equal and are considerably smaller than the next smallest. This indicates that the null space of  $W^T W$  is of rank = 4 as expected from Theorem 1. Simply taking the eigenvector corresponding to the smallest eigenvalue would be a mistake.

Fig. 4b shows the projection of the vectors  $v_1$ ,  $v_2$ , and  $v_3$  on the eigenvectors of the estimation matrix  $W^T W$ . The projections onto the eigenvectors corresponding to the first 23 eigenvalues are close to zero verifying that the vectors  $v_1$ ,  $v_2$ , and  $v_3$  are orthogonal to the first 23 eigenvectors. This verifies part of Theorem 2 which states that the vectors  $v_1$ ,  $v_2$ , and  $v_3$  are in the null space of  $W^T W$  (the remaining four eigenvectors).

Following the algorithm described in Section 2.1, we compute the eigenvalues and eigenvectors of the matrix

$$W^T W - v_1 v_1^T - v_2 v_2^T - v_3 v_3^T.$$

Fig. 4a (bottom) shows the three smallest eigenvalues. The smallest eigenvalue is significantly smaller than the next smallest value, indicating that the null space is now of rank = 1.

#### 4.4.2 Reprojection of Lines Using the Tensor

After recovering the tensor, one can use the tensor to reproject a line given in two images into the third image. In order to test the tensor estimates we used 10 additional lines shown in Fig. 5. Three of the lines lie in the LLC on the left face of the cube. The other seven do not lie on the LLC.

Fig. 5b, Fig. 5c, and Fig. 5d show the reprojection results (dashed lines) together with the original lines (solid lines) overlaid on image 1. One can see that if the set of lines used to estimate the tensor all belong to an LLC, then other lines in the LLC reproject more or less correctly but the reprojection of lines not in the LLC is incorrect (Fig. 5c). On the other hand, reprojection using the tensor computed by taking into account the degeneracy (Fig. 5d) gives results as good as if we had a nondegenerate set of lines to estimate the tensor (Fig. 5b).

## 5 SUMMARY

We have shown that linear methods for estimating motion and 3D structure from lines lead to a degenerate set of equations in the case of a Linear Line Complex. The LLC, a configuration of lines that all intersect a common line in  $\mathcal{P}^3$ , is in fact a common configuration of lines occurring frequently in man-made environments. This degeneracy is due to a bilinear constraint on lines in two views where the constraint equation has a form similar to the epipolar constraint but where lines replace points and the epipoles are replaced by the image of the common line of intersection in the two views. This constraint can be used to determine whether a set of lines belongs to an LLC and enables us to reject outliers using *least median of squares* [7] or other robust estimation methods.

An LLC is not degenerate for nonlinear methods in general. The theoretical analysis leads to a modification of the linear methods that can recover the structure and motion in the LLC case. We have proven that the motion can be recovered up to eight discrete solutions. Empirical evidence shows that the number of solutions can be reduced further to a unique single solution.

We have implemented the algorithm, and experiments with real images verify the theoretical analysis. Although the results using the modified linear algorithm compare favorably with the results obtained using a nondegenerate set of lines, the system at this point is not robust. For example, it requires that lens distortion be taken into account. Further engineering would be involved in making a practical system.

## APPENDIX

### A.1 Mathematical Background and the Trilinear Tensor

Let  $\mathbf{x}$  be a point in 3D space and its projection in a pair of images be  $p$  and  $p'$ . Then  $p = [I; 0]\mathbf{x}$  and  $p' \cong A\mathbf{x}$ , where  $\cong$  denotes equality up to scale. The left  $3 \times 3$  minor of  $A$  stands for a 2D projective transformation of the chosen plane at infinity and the fourth column of  $A$  stands for the epipole (the projection of the center of camera 1 on the image plane of camera 2). In particular, in a calibrated setting the 2D projective transformation is the rotational component of camera motion and the epipole is the translational component of camera motion.

We will occasionally use tensorial notations as described next. We use the covariant-contravariant summation convention: a point is an object whose coordinates are specified with superscripts, i.e.,  $p^i = (p^1, p^2, \dots)$ . These are called contravariant vectors. An element in the dual space (representing hyperplanes—lines in  $\mathcal{P}^2$ ) is called a covariant vector and is represented by subscripts, i.e.,  $s_j = (s_1, s_2, \dots)$ . Indices repeated in covariant and contravariant forms are summed over, i.e.,  $p^i s_i = p^1 s_1 + p^2 s_2 + \dots + p^n s_n$ . This is known as a contraction. An outer-product of two 1-valence tensors (vectors),  $a_i b^j$ , is a 2-valence tensor (matrix)  $c_i^j$  whose  $i, j$  entries are  $a_i b^j$ —note that in matrix form  $C = ba^T$ .

Matching image points across three views will be denoted by  $p, p', p''$ ; the homogeneous coordinates will be referred to as  $p^i, p^j, p^k$ , or alternatively as nonhomogeneous image coordinates  $(x, y)$ ,  $(x', y')$ , and  $(x'', y'')$ —hence,  $p^i = (x, y, 1)$ , etc.

Three views,  $p = [I; 0]\mathbf{x}$ ,  $p' \cong A\mathbf{x}$  and  $p'' \cong B\mathbf{x}$ , are known to produce four trilinear forms whose coefficients are arranged in a tensor representing a bilinear function of the camera matrices  $A, B$ :

$$\mathcal{T}_i^{jk} = v^j b_i^k - v''^k a_i^j \quad (4)$$

where  $A = [a_i^j, v^j]$  ( $a_i^j$  is the  $3 \times 3$  left minor and  $v^j$  is the fourth column of  $A$ ) and  $B = [b_i^k, v''^k]$ . The tensor acts on a triplet of matching points in the following way:

$$p^i s_j^{\mu} r_k^{\rho} \mathcal{T}_i^{jk} = 0 \quad (5)$$

where  $s_j^{\mu}$  are any two lines ( $s_j^1$  and  $s_j^2$ ) intersecting at  $p'$ , and  $r_k^{\rho}$  are any two lines intersecting  $p''$ . Since the free indices are  $\mu, \rho$  each in the range 1, 2, we have four trilinear equations (unique up to linear combinations). If we choose the *standard* form where  $s^{\mu}$  (and  $r^{\rho}$ ) represent vertical and horizontal scan lines, i.e.,

$$s_j^{\mu} = \begin{bmatrix} -1 & 0 & x' \\ 0 & -1 & y' \end{bmatrix}$$

then the four trilinear forms, referred to as *trilinearities* [10], have the following explicit form:

$$\begin{aligned} x'' \mathcal{T}_i^{13} p^i - x'' x' \mathcal{T}_i^{33} p^i + x' \mathcal{T}_i^{31} p^i - \mathcal{T}_i^{11} p^i &= 0 \\ y'' \mathcal{T}_i^{13} p^i - y'' x' \mathcal{T}_i^{33} p^i + x' \mathcal{T}_i^{32} p^i - \mathcal{T}_i^{12} p^i &= 0 \\ x'' \mathcal{T}_i^{23} p^i - x'' y' \mathcal{T}_i^{33} p^i + y' \mathcal{T}_i^{31} p^i - \mathcal{T}_i^{21} p^i &= 0 \\ y'' \mathcal{T}_i^{23} p^i - y'' y' \mathcal{T}_i^{33} p^i + y' \mathcal{T}_i^{32} p^i - \mathcal{T}_i^{22} p^i &= 0 \end{aligned}$$

These constraints were first derived in [10]; the tensorial derivation leading to (4) and (5) was first derived in [12], [13]. The trilinear tensor has been well known in disguise in the context of Euclidean line correspondences and was not identified at the time as a tensor but as a collection of three matrices (a particular contraction of the tensor, correlation contractions, as explained next) [15], [16], [19]. The link between the four trilinear forms and the earlier work on line correspondences was identified later by Hartley [5].

In this paper on linear degeneracy of LLC, we make use of

- 1) properties of tensor slices and
- 2) admissibility constraints.

These two are detailed below.

#### A.1.1 Properties of Tensor Slices

The properties of tensor slices and their taxonomy were first detailed in [14] and further details can be found in [11]. Here we will briefly state the main results. Consider the matrices  $E_{\delta}$ ,  $W_{\delta}$ ,  $G_{\delta}$  arising, respectively, from the following dot products (contractions) of the tensor with some arbitrary vector  $\delta$

$$\delta_k \mathcal{T}_i^{jk}, \delta_j \mathcal{T}_i^{jk}, \delta^i \mathcal{T}_i^{jk}.$$

For example, the matrix  $E_{\delta}$  is formed by  $\delta_1 \mathcal{T}_i^{j1} + \delta_2 \mathcal{T}_i^{j2} + \delta_3 \mathcal{T}_i^{j3}$ . These three types of dot products produce three types of families:  $E_{\delta}$  and  $W_{\delta}$  are *homography* matrices where  $E_{\delta}$  is a collineation mapping view 1 onto view 2 via the plane determined by the center of projection  $C'$  of camera 3 and the line  $\delta$  residing in view 3 (point and a line determined a plane). Likewise,  $W_{\delta}$  is a homography mapping from view 1 onto view 3 via the plane determined by the center of projection  $C$  of camera 2 and the line  $\delta$  residing in view 2.

The matrix  $G_{\delta}$  is a *correlation* matrix mapping the dual image plane (the space of lines) of view 2 onto the space of collinear points in view 3. The set of collinear points in view 3 form a line which is the epipolar line of the point  $\delta$  in view 1. Because  $G_{\delta}$  maps a 2D space onto a 1D space it must be of rank 2, and its null space can be shown to be the epipolar line in view 2 corresponding to  $\delta$  in view 1. Similarly,  $G_{\delta}^T$ , the transpose of  $G_{\delta}$ , maps lines in view 3 onto collinear points in view 2.

When  $\delta$  is chosen to be  $(1, 0, 0)$ ,  $(0, 1, 0)$ , or  $(0, 0, 1)$ , we obtain a basis of three matrices for each contraction type. For example,  $E_{\delta}$  is spanned by  $E_1, E_2, E_3$  which are the slices of the tensor corresponding to  $\delta_k \mathcal{T}_i^{jk}$  where  $\delta$  is  $(1, 0, 0)$ ,  $(0, 1, 0)$ , or  $(0, 0, 1)$ , respectively. These are called *standard homography slices* of the tensor. Similarly,  $G_1, G_2, G_3$  are the *standard correlation slices* of the tensor, i.e.,  $\mathcal{T}_1^{jk}, \mathcal{T}_2^{jk}$ , and  $\mathcal{T}_3^{jk}$ , respectively. The matrices  $G_1, G_2, G_3$  date back to the work on structure from motion of lines [15], [19], where they were first introduced.

### A.1.2 Tensor Admissibility Constraints

The tensor consists of 27 coefficients, yet the number of degrees of freedom cannot exceed 18 for the simple reason that three camera matrices (33 parameters) minus the degrees of freedom associated with a projective basis (15) leaves us with 18. We should therefore be able to describe the tensor with 18 parameters, or conversely, we should be able to find nine algebraic constraints of the tensor coefficients (admissibility constraints). Work on this issue can be found in [3], [9], [1], [14]. We briefly describe below the source and form of those constraints.

The tensor

$$\mathcal{T}_i^{jk} = v^j b_i^k - v''^k a_i^j$$

is determined by 24 parameters given by the two camera matrices, each has 12 parameters. Two additional parameters drop out because we can scale  $v$  and accordingly  $b_i^k$  without changing the tensor, and likewise scale  $v''$  and accordingly  $a_i^j$ . An additional parameter drops out because of the global scale factor (tensor is determined up to overall scale). Thus, we readily see there can be at most 21 parameters defining the tensor. We can drop out three more parameters by noticing that the matrices  $a_i^j$  and  $b_i^k$  belong to a family of homography matrices that leaves the tensor unchanged (uniqueness proof in [10]), as detailed below:

$$\begin{aligned} \mathcal{T}_i^{jk} &= v^j b_i^k - v''^k a_i^j \\ &= v^j (b_i^k + \alpha_i v''^k) - v''^k (a_i^j + \alpha_i v^j) \\ &= \mathcal{T}_i^{jk} + \alpha_i v^j v''^k - \alpha_i v^j v''^k \\ &= \mathcal{T}_i^{jk} \end{aligned}$$

hence, we have three free parameters  $\alpha_i$  (in geometric terms there is a free choice of reference plane in space). We can select  $\alpha_i$  such that the matrix  $b_i^k$  will have a vanishing column (this corresponds to selecting a reference plane coplanar with the center of projection of the third view). Therefore, the new matrices  $a_i^j$  and  $b_i^k$  have only 15 nonvanishing entries, and we have reduced the number of parameters from 21 to 18.

To see where the nine algebraic constraints come from, we revisit the correlation contractions and obtain the following three groups of constraints:

- 1) Rank  $(\delta^i \mathcal{T}_i^{jk}) = 2$  for all choices of  $\delta$ . The three standard correlation slices  $G_1, G_2, G_3$  are of rank 2 each and this property is closed under all linear combinations.
- 2) Since the null space of  $\delta^i \mathcal{T}_i^{jk}$  is an epipolar line, and since all epipolar lines are concurrent, then Rank  $(\text{null}(G_1), \text{null}(G_2), \text{null}(G_3)) = 2$ .
- 3) Similarly, Rank  $(\text{null}(G_1^T), \text{null}(G_2^T), \text{null}(G_3^T)) = 2$ .

One can easily show that no subset of these constraints is sufficient to describe an admissible tensor of the form of (4). The latter two groups represent a six-order polynomial each. To see why this is so note that the null space of rank-2 matrix can be represented by the cross-product of two of its rows—which is a bilinear function of the elements of the matrix. The determinant of the matrix of null spaces of  $G_1, G_2, G_3$  is a cubic function of the bilinear functions of the original elements of the tensor, hence is a sixth-order polynomial of the elements of the tensor.

The first group, when properly counted, yields seven algebraic constraints, three of them of order 3 (determinants of  $G_i$  vanish), and the remaining four are of order 4 (arising from the fact that the vanishing determinant is closed under linear combinations). The derivation of these constraints are beyond the scope of this appendix and will be detailed elsewhere.

### ACKNOWLEDGMENTS

A.S. wishes to thank Steve Maybank, Shai Avidan, and Nassir Navab for helpful comments and acknowledges the financial support from US-IS Binational Science Foundation 94-00120/2, the European ACTS project AC074 "Vanguard," and DARPA through ARL Contract DAAL01-97-0101. G.S. would like acknowledge the financial support from ONR contract N00014-94-1-0128 and DARPA contracts N00014-94-01-0994 and N00014-97-0363.

### REFERENCES

- [1] S. Avidan and A. Shashua, "Tensorial Transfer: On the Representation of  $n > 3$  Views of a 3D Scene," *Proc. DARPA Image Understanding Workshop*, Palm Springs, Calif., Feb. 1996.
- [2] T. Buchanan, "On the Critical Set For Photogrammetric Reconstruction Using Line Tokens in p3(c)," *Geometriae Dedicata*, vol. 44, pp. 223-232, 1992.
- [3] O.D. Faugeras and T. Papadopoulos, "A Nonlinear Method for Estimating the Projective Geometry of Three Views," *Proc. Int'l Conf. Computer Vision*, Bombay, India, Jan. 1998.
- [4] R.I. Hartley, "In Defense of the 8-Point Algorithm," *Proc. Int'l Conf. Computer Vision*, June 1995.
- [5] R.I. Hartley, "Lines and Points in Three Views and the Trifocal Tensor," *Int'l J. Computer Vision*, vol. 22, no. 2, pp. 125-140, 1997.
- [6] S.J. Maybank, "The Critical Line Congruence for Reconstruction From Three Images," *Applicable Algebra in Engineering Communication and Computing*, vol. 6, pp. 89-113, 1995.
- [7] P. Meer, D. Mintz, D. Kim, and A. Rosenfeld, "Robust Regression Methods for Computer Vision: A Review," *Int'l J. Computer Vision*, vol. 6, no. 1, pp. 59-70, 1991.
- [8] N. Navab, O.D. Faugeras, and T. Vieville, "The Critical Sets of Lines for Camera Displacement Estimation: A Mixed Euclidean-Projective and Constructive Approach," *Proc. Int'l Conf. Computer Vision*, Berlin, May 1993.
- [9] T. Papadopoulos and O.D. Faugeras, "A New Characterization of the Trifocal Tensor," *Proc. European Conf. Computer Vision*, Freiburg, Germany, June 1998.
- [10] A. Shashua, "Algebraic Functions for Recognition," *IEEE Trans. Pattern Analysis and Machine Intelligence*, vol. 17, no. 8, pp. 779-789, Aug. 1995.
- [11] A. Shashua, "Trilinear Tensor: The Fundamental Construct of Multiple-View Geometry and Its Applications," G. Sommer and J.J. Koenderink, eds., *Algebraic Frames for the Perception Action Cycle*, no. 1,315 in Lecture Notes in Computer Science. New York: Springer, 1997. Proceedings of the workshop held in Kiel, Germany, Sept. 1997.
- [12] A. Shashua and P. Anandan, "The Generalized Trilinear Constraints and the Uncertainty Tensor," *Proc. DARPA Image Understanding Workshop*, Palm Springs, Calif., Feb. 1996.
- [13] A. Shashua and S. Avidan, "The Rank4 Constraint in Multiple View Geometry," *Proc. European Conf. Computer Vision*, Cambridge, UK, Apr. 1996.
- [14] A. Shashua and M. Werman, "Trilinearity of Three Perspective Views and Its Associated Tensor," *Proc. Int'l Conf. Computer Vision*, June 1995.
- [15] M.E. Spetsakis and J. Aloimonos, "Structure From Motion Using Line Correspondences," *Int'l J. Computer Vision*, vol. 4, no. 3, pp. 171-183, 1990.
- [16] M.E. Spetsakis and J. Aloimonos, "A Unified Theory of Structure From Motion," *Proc. DARPA Image Understanding Workshop*, 1990.
- [17] G. Stein and A. Shashua, "Model Based Brightness Constraints: On Direct Estimation of Structure and Motion," *Proc. IEEE Conf. Computer Vision and Pattern Recognition*, Puerto Rico, June 1997.
- [18] G. Stein, "Lens Distortion Calibration Using Point Correspondences," *Proc. IEEE Conf. Computer Vision and Pattern Recognition*, Puerto Rico, June 1997.
- [19] J. Weng, T.S. Huang, and N. Ahuja, "Motion and Structure From Line Correspondences: Closed Form Solution, Uniqueness and Optimization," *IEEE Trans. Pattern Analysis and Machine Intelligence*, vol. 14, no. 3, Apr. 1992.